Study of Electronic, Optical and Magnetic Properties of Doped and Un-Doped Double Transition Metal MXenes Using Density Functional Theory

Syed Haider Ali
Reg. No: 328717

A thesis submitted in partial fulfillment of the requirements. for the degree of **Master of Science**
in
Physics

Supervised by: Prof. Dr. Syed Rizwan Hussain

Department of Physics
School of Natural Sciences
National University of Sciences and Technology
H-12, Islamabad, Pakistan
Year 2022
Study of Electronic, Optical and Magnetic Properties of

THESIS ACCEPTANCE CERTIFICATE

Certified that final copy of MS thesis written by **Syed Haider Ali** (Registration No. **00000328717**), of **School of Natural Sciences** has been vetted by undersigned, found complete in all respects as per NUST statutes/regulations, is free of plagiarism, errors, and mistakes and is accepted as partial fulfillment for award of MS/M.Phil degree. It is further certified that necessary amendments as pointed out by GEC members and external examiner of the scholar have also been incorporated in the said thesis.

Signature: _____

Name of Supervisor: Prof. Syed Rizwan Hussain

Date: 04-05-2023

Signature (HoD): _____

Date: 04-05-2023

Signature (Dean/Principal): _____

Date: 05.05.2023

FORM TH-4

National University of Sciences & Technology

MS THESIS WORK

We hereby recommend that the dissertation prepared under our supervision by: **"Syed Haider Ali"** Regn No. **00000328717** Titled: **"Study of Electronic, Optical and Magnetic Properties of Doped and Un-Doped Double Transition Matel MXenes Using Density Functional Theory"** accepted in partial fulfillment of the requirements for the award of **MS** degree.

Examination Committee Members

1. Name: DR. FAHEEM AMIN Signature: _____

2. Name: DR. FOUZIA PARVEEN MALIK Signature: _____

Supervisor's Name: PROF. SYED RIZWAN HUSSAIN Signature: _____

_____ 04-05-2023

Head of Department Date

COUNTERSINGED

Date: 05.05.2023 _____

Dean/Principal

Declaration

I certify that this research work titled "*Study of Electronic, Optical and Magnetic Properties of Doped and Un-Doped Double Transition Metal MXenes. Using Density Functional Theory"* is my own work. The work has not been presented elsewhere for assessment. The material that has been used from other sources it has been properly acknowledged / referred.

Signature of Student

Syed Haider Ali Zaidi

2020-NUST-MS-Phy-328717

Plagiarism Certificate (Turnitin Report)

This thesis has been checked for Plagiarism. Turnitin report endorsed by Supervisor is attached.

Signature of Student
Syed Haider Ali Zaidi
Registration Number 328717

Copyright Statement

- Copyright in text of this thesis rests with the student author. Copies (by any process) either in full, or of extracts, may be made only in accordance with instructions given by the author and lodged in the Library of NUST School of Natural Sciences (SNS). Details may be obtained by the Librarian. This page must form part of any such copies made. Further copies (by any process) may not be made without the permission (in writing) of the author.

- The ownership of any intellectual property rights which may be described in this thesis is vested in NUST School of Natural Sciences, subject to any prior agreement to the contrary, and may not be made available for use by third parties without the written permission of the SNS, which will prescribe the terms and conditions of any such agreement.

- Further information on the conditions under which disclosures and exploitation may take place is available from the Library of NUST School of Natural Sciences, Islamabad.

Acknowledgements

My heartfelt gratitude goes to my loving parents who have been a constant source of support and encouragement, not just during my studies, but throughout my entire life. Their unwavering patience and guidance have enabled me to reach where I am today.

I would also like to extend my sincere thanks to my supervisor, **Professor Dr. Syed Rizwan Hussain**, for expertly guiding me through the thesis process and providing invaluable assistance at every step. A special note of appreciation goes to **Dr. Fouzia Perveen Malik** and **Dr. Faheem Amin** for their insightful suggestions and guidance in the computational aspect of my research. I am also grateful to the principal of the School of Natural Sciences, **Prof. Dr. Rashid**, for their supportive suggestions throughout my program.

Lastly, I cannot express enough gratitude to **Dr. Saleem Ayaz** Khan for his invaluable support and guidance throughout my research journey.

Dedicated to

My Parents

And

My Sister

Abstract

$Mo_2TiC_2T_x$ is a part of the ever-growing family of MXenes and lies in the category of double transition metal MXenes. The aim of this study was to explore the various properties of this MXene such as electronic band structure, density of states, magnetic moment, and optical properties. Density functional theory was used to model all of these properties for unmodified and modified structure with 4% Niobium (Nb) doping. Both systems under study had 0 eV band gap indicating a good conductivity. Pristine system was found to be non-magnetic, but the doping resulted in the introduction of magnetic moment into the system up to 4.0 μ_B. All the optical properties of both materials show almost a similar trend. Both systems display an ascending trend of absorption, and due to this it can be predicted that both materials can potentially have applications in solar cell fabrication.

Table of Contents

List of Figures

List of Tables

Chapter 1
Introduction

1.1 MXenes and Their Types

MXenes are the family of 2D transition metal carbides, nitrides or carbonitrides. They have found their applications in energy storage systems, Li-ion batteries, and water purification. Due to their flexibility, high conductivity, and ease of processing they are extremely desirable in the process of EMI shielding [1].

MXenes have the general formula of $M_{n+1}X_nT_x$ where T_x represents the functional groups attached, and they are etched from MAX phases which have the general formula of $M_{n+1}AX_n$. Here, M is the transition element e.g., Ti, Mo, V etc. A belongs to the group A elements e.g., Si, Al, In, etc. and X is Carbon/Nitrogen or both. They are hexagonal in structure with P63/mmc symmetry. The results after intercalation of different salts and organic compounds with MXenes has shown very promising results for applications in electronic devices, sensors, energy storage devices [2].

By now several different compositions of MXenes have been discovered, and with the passage of time more and more of them are being added to this ever-growing family of these 2D materials. They can be classified into three different types.

1.1.1. Mono Transition Mental MXenes

After the group A metallic layer is etched out from the MAX phase, we get the MXenes with chemical composition of $M_{n+1}X_n$. If the M layer is made up of only one type of transition element, then the type of MXene can be categorized as Mono Transition. The examples for these are Ti_3C_2, V_2C, and Nb_2C [3].

1.1.2 Double Transition Metal MXene

Unlike the previous one, if there are two different types of transition elements forming a layer respectively then we can classify that type of MXene as a double transition MXene. Some of the examples for this are Mo_2TiC_2, $Mo_2Ti_2C_3$ and Mo_4VC_4. The general formula for this type of MXenes in the solid solution is $(M'_{2-y}M''_y)\ C$, $(M'_{3-y}M''_y)\ C_2$, $(M'_{4-y}M''_y)\ C_3$, or $(M'_{5-y}M''_y)\ C_4$ [4]. This research focuses on different properties of this type of MXenes.

1.1.3. Divacancy MXenes

With the advancement in the study of MXenes, this is the new type which has been recently discovered. The experiment for this involved the synthesis of a 3D atomic laminated structure of $(Mo_{2/3}Sc_{1/3})_2A1C$, and the selective etching of the Al and Si atoms [5].

1.2. Synthesis of MXenes

The synthesis of MXenes usually requires an etching solution like HF, which helps in etching out the metallic layer from the MAX phase.

Etching is a process that utilizes liquid chemicals or etchants to remove materials from the wafer by forming soluble by products. Substrate in this process is dipped in etchant. The methods involve three main steps [3]:

- Diffusion of liquid etchant towards the material that is required to be removed.
- The reaction that occurs between the etchant and the element to be removed away. Usually at this stage a redox reaction takes place. This reaction involves the oxidation of the element which needs to be removed away and then dissolution of the oxides in the given etchant.
- Diffusion of by products from the substrate. The by-products formed are soluble and therefore can be taken away during washing.

1.3 Mo_2TiC_2-T_x MXene

It also has a layered structure in which the Mo layer occupies the space between Titanium and the Carbon layers.

1.3.1 Synthesis

For the synthesis following steps are followed [3].

1. Mo_2TiAlC_2 powder is slowly added to the 48% to 50% HF solution.
2. The ratio between MXene and HF solution should be 1:10.
3. The solution should be kept at 55℃ and continuously stirred for 48hrs.
4. The solution is then washed with centrifugation at 3500 rpm.

1.3.2 Applications

As they belong to the family of MXenes they possess many of the commonly shared properties such as high thermal and electrical conductivity, and remarkable volumetric capacitance [5]. Apart from this following are some of the areas for which they have found their applications in.

1. Long life and high power of the Li-ion and Sodium-ion batteries[6].
2. Catalyst for electro catalytic synthesis of Ammonia[7].
3. Achieving ultra-high ductility and fracture resistance in Mo-alloys [7].

Chapter 2

Literature Review

Today computers have found their applications in the study of materials. With the help of different computation techniques, we can study various properties of materials without the need of hit and trial experiments and this is a very cost-effective approach to the study of materials. The computational study incorporates different theories from theoretical condensed matter physics for example DFT and DMFT (Dynamic Mean Field Theory). The theoretical study of materials does not require prior knowledge of the system. This chapter will be focused on Density Functional Theory (DFT).

2.1 Density Functional Theory

With DFT we can successfully study the properties of materials on a quantum mechanical level. The electronic structure properties, optical properties and magnetic properties can be successfully calculated with DFT up to close approximation to the experimentation. Ground state properties of the materials are measured with the help of ground state charge density, which is a function of the ground state electron wave function. For solving such many body systems, we need to look beyond the Schrodinger Wave Equation (SWE) because with the increase of electrons and different atoms, the number of variables increases thereby increasing the complexity of solving SWE.

2.1.1 Schrodinger Wave Equation and Many Body Systems

SWE was developed by Erwin Schrödinger in 1926 that described the wave function of a system, which contained all its information.

$$\left[\frac{\hbar^2}{2m} + V_{KS}\right]\Psi(r) = E\Psi(r) \qquad \textbf{(2. 1)}$$

Here $\frac{\hbar^2}{2m}$ represents the kinetic energy of the system and V(r) represents the potential energy. These two combines to give us the Hamiltonian operator. $\Psi(r)$ is the wavefunction of the quantum mechanical system.

For many-body system, the above equation gets modified. All possible interactions are considered in it and then the Hamiltonian takes the following form.

$$H = -\frac{1}{2}\sum_i \nabla^2 - \sum_A \frac{1}{2M_A}\nabla^2 - \sum_{A,i}\frac{Z_A}{r_{Ai}} + \sum_{A>B}\frac{Z_A Z_B}{R_{AB}} + \sum_{i>j}\frac{1}{r_{ij}} \quad \textbf{(2. 2)}$$

$$H = \boldsymbol{T_N(R)} + \boldsymbol{T_e(r)} + \boldsymbol{V_{eN}(r,R)} + \boldsymbol{V_{NN}(R)} + \boldsymbol{V_{ee}(r)} \quad \textbf{(2. 3)}$$

Here i, j refer to electrons and A,B refer to nuclei. Here we can see the first two terms as independent kinetic energies of electrons and nuclei respectively. The third term depicts the interaction between nuclei and the electron. In the fourth term nuclei-nuclei interaction is represented and the final term is of electron-electron interaction.

To solve this many-body system, Born-Oppenhimer approximation is used where the nuclei are considered static compared to the electrons due to larger mass, thus their kinetic energies are omitted.

Thus, we have the following expression.

$$H = \boldsymbol{T_e(r)} + \boldsymbol{V_{eN}(r;R)} + \boldsymbol{V_{NN}(R)} + \boldsymbol{V_{ee}(r)} \quad \textbf{(2. 4)}$$

2.1.2 Hartree-Fock (HF) Theory

SWE has its limitations when it comes to calculate wave function for many-body systems. Thus, after Born-Oppenhimer approximation Hartree Fock is of great importance. The HF method is also known as the **Self Consistent Field (SCF)** because this approach leads us to an approximate solution of the Schrodinger Equation and the field computed from a particular charge distribution should be consistent with the initially assumed field.

In this approach the electrons experience an average electrostatic field and can move freely. This method makes the use of vibrational principle to calculate the ground state wave function and the ground state energy. From here we can find different properties of the system under consideration.

$$E_{ground} \leq \langle \Psi | \mathbf{H} | \Psi \rangle \quad (2.5)$$

The first step is to guess the wave function and calculate the respective ground state energy. Then the process is repeated until the approximate energy and wavefunction are found which are consistent with the guessed wave function. Through this iterative procedure we can reach **self-consistency.** Although the SCF method provides us an easy solution for the many-body systems problems, the results obtained from this method are very impractical, because there is no account for the electron's spin. Due to this we can't accurately predict many different properties.

2.1.3 Electron Density

As the name suggests, electron density is the main variable for DFT, and it plays a fundamental role. Therefore, it is necessary to explain it.

$$\rho(r) = N \int \dots \int |\Psi(x_1, x_2, \dots, x_N)|2 \, ds_1 dx_2 \dots dx_N \quad (2.6)$$

$$\rho(r) = N \sum s_1 \dots \sum s_N \int dr_2 \dots \int dr N \, |\Psi(r_1, s_1, r_2 s_2, \dots, r_N s_N) \quad (2.7)$$

$$\rho(r) = \langle \Psi | \hat{\rho}(r) | \Psi \rangle \quad (2.8)$$

where the operator is:

$$\hat{\rho}(r) = \sum_{i=1}^{N} \sum_{si} \delta(r - r_i) \quad (2.9)$$

Here **r** and s represent the position and spin respectively. After taking the integral over the wavefunction we will have the probability density of an electron for a specific volume element.

2.1.4 Thomas Fermi Model

DFT was initially proposed in 1927 by Thomas and Fermi. This approach assumed electrons around the nucleus to form homogeneous electron gas. The electron gas followed the fermi-Dirac statistics, and the potential used for electron-electron interaction was the classic coulomb potential. Local density approximation (LDA) was used to determine the kinetic energy of the system. The energy of the system is a function of the electron density and takes the following form.

$$E_{TF}[\hat{\rho}(r)] = A_1 \int \hat{\rho}(r)^{5/3} dr + \int \hat{\rho}(r) V_{ext}(r) dr + \int\int \frac{\hat{\rho}(r)\hat{\rho}(r')drdr'}{|r - r'|} \quad (2.10)$$

This is the energy of the system under the external potential, where the first term represents the kinetic energy with A_1 being the constant value as $\mathbf{A_1 = 310(3\pi^2)^{2/3}}$. The second term represents the interaction between the electrons and the nuclei. The last term represents the electron-electron coulomb interaction.

Although this was the first step towards the advancements in DFT, the theory had many complications due to which it wasn't applicable. The model doesn't give any kind of explanation about the bonding between the atoms; thus, the molecular formation is not possible. It does not incorporate the exchange potential, furthermore the total spin of homogeneous electron gas may or may not be zero, because the number of spins up and spin down electrons are unclear.

2.1.5 Kohn-Sham Equations

In this system, the electron density of interacting system is generated for the fictitious system of non-interacting electrons. The problem of many body systems was further reframed by Kohn and Sham. The system of interacting electrons was mapped on to a system of non-interacting electrons with the same ground state density and energy[8]. Although the electrons don't interact explicitly, but they interact by the field generated by other electrons.

The external potential is represented as VKS, which corresponds to the non-interacting electrons. The wave function is in the form off slater determinant which will have the lowest energy solution because of no interaction among the particles. In general, the exact Hamiltonian of the electron is:

$$H_{el} = \sum_{i=1}^{Nel} -\frac{1}{2}\nabla^2 + \sum_{i=1}^{Nel}\left[\sum_{A=1}^{Nat} \frac{-Z_A}{|r_i - R_A|}\right] + \sum_{i=1}^{Nel}\sum_{j=i+1}^{Nel} \frac{1}{|r_i - r_j|} \quad (2.11)$$

$$= \sum_{i=1}^{Nel} -\frac{1}{2}\nabla^2 + \sum_{i=1}^{Nel} V_{ext} + \sum_{i=1}^{Nel}\sum_{j=i+1}^{Nel} \frac{1}{|r_i - r_j|} \quad (2.12)$$

Here we can see that due to the coulomb interaction the equation can't be separated into independent ri and r_j terms. Contrary to this, the equation for the KS system will be as follows.

$$H_{KS}\Psi_i(r) = \left\{\frac{-h^2}{2m}\nabla^2 + V_{KS}(r)\right\}\Psi_i(r) \quad (2.13)$$

$$= \varepsilon_i\Psi_i(r) \quad (2.14)$$

V_{ks} exists uniquely at the ground state density (r). The orbital energy is represented by ϵ. The density of this N-particle system will be represented as follows.

$$\hat{\rho}(r) = \sum_{i}^{N} |\Psi_i(r)|^2 \quad (2.14)$$

The total energy can be written as:

$$E[\rho(r)] = T_{KS}[\rho(r)] + U[\rho(r)] + E_{xc} + \int \rho(r)V_{KS}dr \quad (2.15)$$

Where $T_{KS}[\rho(r)]$ is the kinetic energy functional of the non-interacting system such that,

$$T_{KS}[\rho(r)] = \langle\psi i(r)|T|\psi i(r)\rangle \quad (2.16)$$

Furthermore, the density remains the same that is $\int \rho_{(r)}dr = N$.

$[(r)]$ is called as the exchange correlation function, this is responsible for the compensation of the missing energy due to our approximation of non-interacting electrons. The ground state of the system can be obtained by minimizing the energy functional using the vibrational principle.

$$\frac{\delta}{\delta\rho(r)}\left[E[\rho(r)] - \mu\int \rho(r)dr\right] = 0 \quad (2.17)$$

Were μ is the Lagrange multiplier, which then takes the value:

$$\frac{\delta E[\rho(r)]}{\delta\rho(r)} = 0 \quad (2.18)$$

Thus,

$$\frac{\delta T_{ks}[\rho(r)]}{\delta\rho(r)} = V_{KS}(r) = \mu \tag{2.19}$$

K_S potential will become as following:

$$V_{KS}(r) = V(r) + \frac{\delta U[\rho]}{\delta\rho} + \frac{\delta E_{xc}[\rho]}{\delta\rho} \tag{2.20}$$

$$V_{ks} = V(r) + V_H(r) + V_{xc}(r) \tag{2.21}$$

V_H is the Hartree potential.

$$V_H = \int \frac{\rho(r')}{r - r'} dr \tag{2.22}$$

And V_{xc} is the exchange correlation potential.

$$V_{xc}(r) = \frac{\delta E_{xc}[\rho]}{\delta\rho} \tag{2.23}$$

2.1.6 Summary of Kohn-Sham DFT

1. Initially, electron density ((r)) needs to be assumed.
2. VKS is computed for this electron density.
3. Then the non-interacting Schrodinger equation is computed to get the wavefunction of the system.
4. Then the density is computed with the help of this wavefunction.
5. We repeat this process until the results converge i.e., the computed charge density is equal to the assumed charge density then we have.

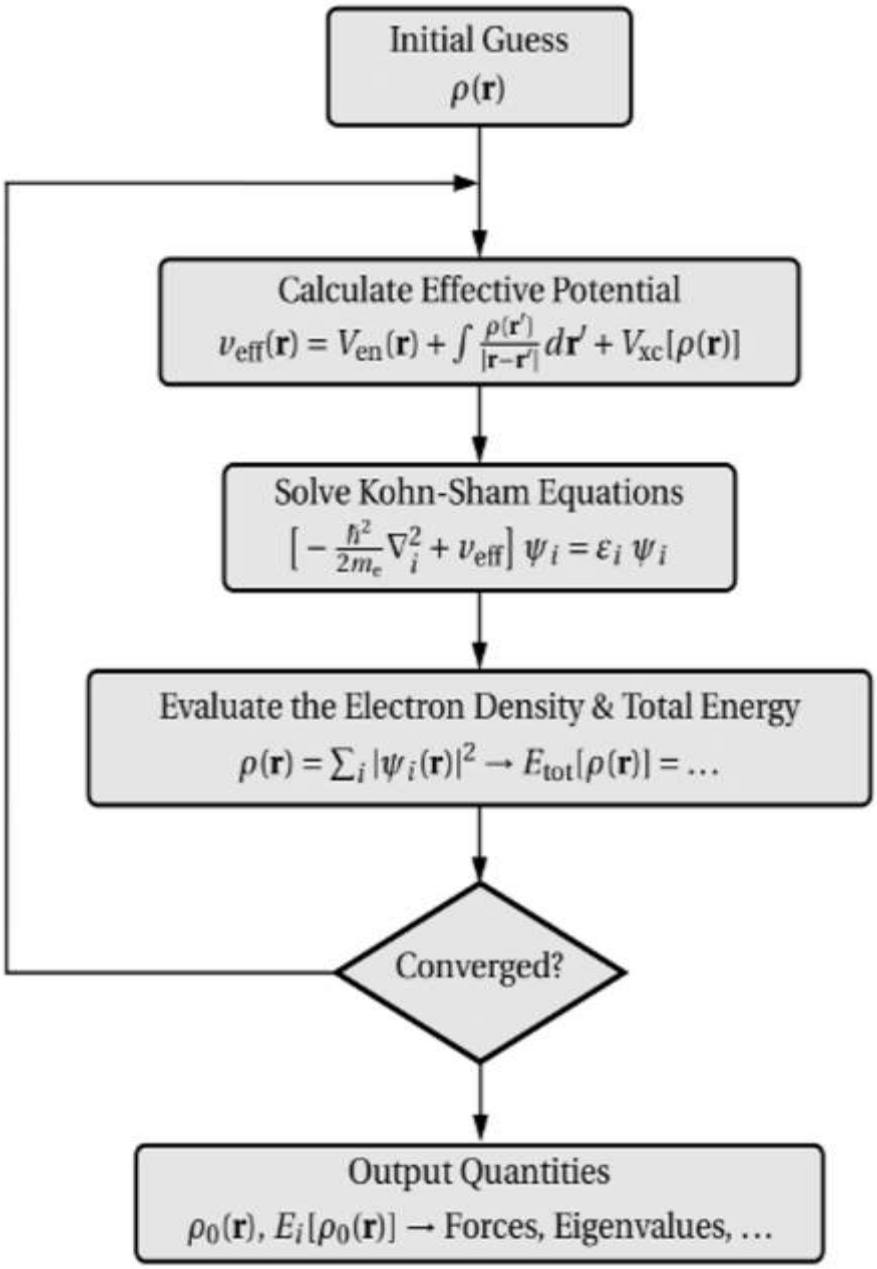

***Figure 2.1**: Schematic Diagram of a Self-Consistent Field cycle*[9] .

2.2 Exchange-Correlation Potential

A system of electrons has an antisymmetric wave function, thus the exchange of the position of electrons can result in the change of the system i.e., with a negative sign[10]. This gives rise to the exchange energy in the system which can be represented as.

$$E_X = -\int\int \Psi_i(r_1)\Psi_j(r_j)\frac{1}{r_{12}}\Psi_i(r2)\Psi_j(r1)\, dr_1 dr_2 \qquad (2.24)$$

This correlation comprises all the unknown parts of the energy of the original many body systems.

The most used exchange correlation functionals are Local Density Approximation (LDA), Local Spin Density Approximation (LDSA), and Generalized Gradient Approximation (GGA).

$$E_{xc} = \int \rho(\mathrm{r})\varepsilon_{xc}(\rho(\mathrm{r})) \tag{2.25}$$

$$E_{xc} = E_x + E_c \tag{2.26}$$

$$E_x = \int \rho(\mathrm{r})\varepsilon_x(\rho(\mathrm{r})) \tag{2.27}$$

$$E_c = \int \rho(\mathrm{r})\varepsilon_c(\rho(\mathrm{r})) \tag{2.28}$$

2.2.1 Local Density Approximation

It is one of the earliest approaches towards the xc functionals [13]. The system is considered to have homogeneous electron gas (HEG). The exchange functional has been computed analytically.

$$E_x^{LDA}[n] = \frac{3}{4}\left(\frac{3}{\pi}\right)^{1/3} \int n(r)^{4/3}\, dr \tag{2.29}$$

The correlation energy functional is then defined with the help of quantum monte Carlo simulations. On the other hand, Local Spin Density Approximation (LSDA) also incorporates the spin of electrons [12].

2.2.2 Generalized Gradient Approximation

LDA has its limitations. The free electron gas might give better results regarding properties of metals, but it is not a suitable approximation for semiconductors and insulators[11]. Thus, in GGA the electron cloud is assumed to be spread in the form of a gradient[12].

$$E_{xc}^{GGA} = \int f_{xc}^{GGA}\left(\rho_\alpha, \rho_\beta, \nabla\rho_\alpha, \nabla\rho_\beta\right) dr \tag{2.30}$$

To get better results compared to LDA approximation, we need to make the xc functional depend on the density of the electron as well as the gradient of the density of electrons. There are many approaches towards GGA functionals which include PBE, P86, B88, and LYP.

The results that are obtained by solving KS equations using GGA are usually better than the ones obtained through LDA. Some of the GGA's that are derived by different scientists and revised as well are mentioned [12].

2.2.3 Exchange-Correlation Beyond LDA and GGA

The approximations towards exchange correlation functional are not only till GGA and LDA but beyond this we have the hybrid functionals and Hubbard potential as well. Hybrid functional are combination of two functional e.g., B3LYP is a combination of BP and LYP GA functional, and PBE0 is a combination of Hartree exchange energy, PBE-GGA exchange energy and PBE-GGA correlation energy.

Hubbard potential had been introduced after the failure of GGA and LDA functionals to calculate some properties of compounds like Mott insulators and magnetism in compounds with d and f orbitals. This led to the use of Hubbard potential in DFT, which includes the missing measures of the columbic on-site interaction. In 1963, Hubbard introduced the interaction to explain the ferromagnetism for a compound in Hartree theory. According to Hubbard, considering ferromagnetism of an atom for its ground state, the anti-parallel state of an electron exists, which is not possible under Fermi-Dirac statistics as electron are fermions and two electrons cannot have the same spin. Hence, the Hubbard potential was introduced to KS-DFT later by Anisimov et al. in 1991[13]. They had bridged the gap between DFT and Hubbard potential to be able to calculate magnetism and other properties correctly. This gave the functional the form LDA+U, GGA+U etc. where U indicates the Hubbard potential. There have been various studies for the value of U when calculating properties, as its value changes according to the number of electrons in the compounds, usually U has value between 1 eV to 10 eV, 10 eV being the highest value.

Chapter 3

Wien2k

In this thesis for DFT calculations, computer program WIEN2k is used written in FORTRAN. The original developers of WIEN2k are Peter Blaha and Karlheinz Schwarz of the institute of Materials Chemistry, Vienna University of Technology [17]. The first release of the program was in 1990's and was updated over the years i.e. WIEN93, WIEN97, and then WIEN2k. WIEN2k allows us to compute many properties of a structure using the full potential linearized augmented plane wave method for the basis set. The choice of basis set and plane wave method is discussed in the subsection. While the simulation method and the different properties that can be calculated through WIEN2k are also mentioned. It can also be used for best calculation of band structure. In WIEN2k programs are linked through c-shell scripts, so it should operate in the Linux environment.

3.1 Choice of Basis Set and Wave function

For solving DFT, there are many different codes depending on different wave functions and basis sets. The most used method for solving the structures is the linear combination of atomic orbitals (LCAO) while the orbital is used in Gaussian or Slater formulation. Furthermore, muffin tin approximation (MTA) is also used, where the potential and charge density inside the atomic sphere are spherically symmetric and for outside the sphere has a constant value for atoms in the crystal. Properties that are dependent more on the calculations of density near the nucleus of an atom are to be explained through an all-electron wave function. All electron functions contain the complete information of the wave function [14]. There are three basic schemes that has been suggested for the plane wave functions i.e., Augmented Plane Wave (APW), Linear Augmented Plane Wave (LAPW) and Augmented Plane Wave with local orbitals (APW+LO).

3.1.1 Augmented Plane Wave Method

In 1937, Slater developed the APW method, in which MTA is used, such that the near a nucleus the potential and wave function is the same as the one inside the atom but for the interstitial positions the potential and wave functions are consistent and level [15]. Based on this analysis the space in a compound is studied in two regions i.e., the non-overlapping

spheres that make up the muffin tin and the overlapping spherical area is considered as the interstitial region shown as region I and II in figure 3.1. Where for the expansion of muffin tin region the radial solutions for the SWE are considered.

$$\Psi(\mathrm{r}) = \begin{cases} \left\{\frac{1}{\sqrt{\Omega}}\sum_{G} c_G r^{i(G+k).r}, & r \epsilon I \\ \sum_{lm} A_{lm} u_l(r) Y_{lm}(r), & r \epsilon S \end{cases} \qquad (3.1)$$

where wavefunction ψ, Ω the cell volume, and ul is the regular solution of equation.

$$\left[\frac{d^2}{dr^2} + \frac{l(l+1)}{r^2} + V(r) - E_l\right] r u_l(r) = 0 \qquad (3.2)$$

Here, cG and Alm are coefficients for expanding the wave function, El is a parameter, V is the spherical component of the potential in the region I.

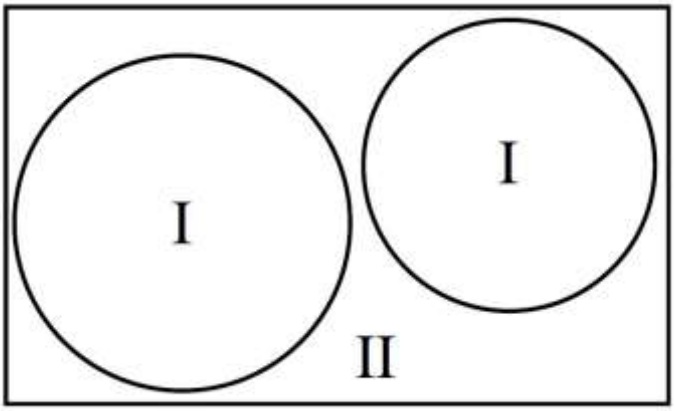

Figure 3. 1: *Atomic muffin tin region I and interstitial region II [16]*

However, the problem with APW method is that the energies are not the same on the bounties as (r) is zero on the boundary which will be a problem in general for elements with d and f orbitals. [15]. An additional problem while using APW is its extension to a general crystal potential and removing the limitation of MTA [15, 16]. For the purpose of avoiding the APW method and its problems with the energy, Anderson and Abraham et al [17, 18] gave

the linearized plane wave methods called as Linear Augmented Plane Wave method (LAPW) . This is the LAPW method, for which inside the spheres, linear combinations of radial functions, $(r)(\hat{r})$and their derivatives with respect to the linearization parameters are used as basic functions, El. The (r) is the same as used in the APW method in with a fixed El, where the equation is modified and given as

$$\psi(\mathrm{r}) = \begin{cases} \frac{1}{\sqrt{\Omega}} \sum_G c_G e^{i(G+k).r}, & r \epsilon I \\ \sum_{lm} [A_{lm} u_l(r) + B_{lm} u_l(r) Y_{lm}(r)], & r \epsilon S \end{cases} \quad (3.3)$$

In equation B is the coefficient for the energy derivative and similar in meaning to Alm. For the interstitial region of LAPW, the wave function is the same as APW while correction is done mainly to inside the sphere wave function.

This correction solves the issue in the APW method along with giving a PW method with increased accuracy for obtaining band structure and other properties while MTA was still used [16].

3.1.2 APW+LO and LAPW+LO

Besides APW and LAPW method, there is one more extension of adding the correction to semi core states for better computation. This addition is completely for the localized orbitals inside the muffin tin spheres such that their values become zero at the boundary of muffin tin spheres. Hence, no other boundary condition dependent wave function is introduced [17]. The three functions (r), $\dot{u}(r)$ and $ulo(r)$ are all present together for the muffin tin sphere part of the wave function, while making sure that the derivative of local orbital is zero at the boundary. Moreover, though LO was introduced for treatment of semi-core electrons, the LAPW+LO scheme introduces correction to the electrons present in the higher states as well i.e., that are much above the range of energy parameters El of LAPW. These are difficult to be described with decent accuracy and hence the extended LAPW+LO method is used which is also discussed by Krasovskii and Schattke[17,18] in the extended LAPW method. The LAPW+LO basis functions are:

$$\psi_{l(r)} = \sum_m A_{lm}^{lo} u_l(r) + B_{lm}^{lo} u_l Y_{lm}(r) \quad (3.4)$$

In this equation the coefficients A_{lm}^{lo} and B_{lm}^{lo} are picked such that the boundary condition for local orbitals in MTA is satisfied.

While MTA is good considering structure with high periodicity and closely packed ones, they become unlikely to be used for 2D structure or layered compounds and semiconductors. To avoid these approximations for better calculations the full potential (FP) scheme is used in which charge density and potential density are expanded using the Fourier Series and lattice harmonics for interstitial and inside sphere calculations respectively which is further explained in the following subsection[15].

3.1.3 The Full-Potential – LAPW

The combination of full potential scheme with the LAPW method gives us the FP-LAPW method, where FP is used in LAPW method instead of MTA which treats the structure without giving it any specific shape i.e., spherical [21, 22]. This simplification is attained by relaxing the constant interstitial potential $VIo$and the spherical MTA potential $V_{MT}^{L}$by the inclusion of interstitial potential $\sum_G V_G^I\, e^{iGr}$ and the other terms inside the mufn-tin spheres:

$$V(r) = f(x) = \begin{cases} \sum_G V_G^I\, e^{iGr}, & r \in I \\ \sum_L V_{MT}^L\,(r), & r \in S \end{cases} \tag{3.5}$$

This technique used for arriving to this method is the derivation of such a coulomb potential that gives the general charge density without assuming any shape approximations and he charge density is written in a similar manner as in equation 4.31 by replacing V with (r).

FP-LAPW is considered as one of the most accurate and precise methods for determining electronic structures for crystals by solving the equations (Kohn-Sham) of DFT. FP-LAPW is employed in the computer code for example in WIEN2k to study crystal properties on the atomic scale[19].

3.2 Simulations and Properties

To run simulations on WIEN2k program one should make sure that WIEN2k software has been successfully installed on Linux operating system. So now different structures and materials can be simulated. However, a graphical user interface (GUI) is also available for new users. The first step is to simulate a structure using the space group and atomic constants then proceed towards initialization which generates the input files. Afterwards according to the property need to calculate, different commands can be given, and the output files are analyzed for the results.

Currently Kohn-Sham Density functional theory is the most favorable and effective method for computing the electronic structure of matter and its properties by employing quantum mechanics. The fields on which DFT can be applied is a wide range, including simple atomic structures, bulk structure, 2D surfaces, slabs etc. A few of the applications of DFT are:

- An easy way of theoretically verifying and justifying the lattice parameters of a certain material by using different approximations according to the material.
- For studying the electron density, to observe the amount of charge transferred between the atoms in the material
- The band structure of the most complex materials can even be obtained by using DFT and then the direct and indirect bandgaps can be calculated for further study.
- The density of states(DOS) of any material can be observed, including the partial DOS due to any orbital i.e. s, p, d, f, and, depending on the k-mesh and the approximation used finer DOS can be studied
- The optical properties of a material can be studied by calculating the optical parameters of a material i.e., refractive index, optical conductivity, optical reflectivity, optical dielectric constant.
- DFT can be used to study the phonon-electron interactions of a molecule.
- For studying the piezoelectric properties of a material, the spontaneous polarization, piezoelectric tensors, piezoelectric constants, and born effective charges can be calculated by the use of DFT
- The X-Ray spectroscopy can be done for any material using DFT simulations.
- The magnetic properties of different samples can be determined and calculated i.e. magnetic moment, the spin up/down density.

Chapter 4

Results and Discussions

This chapter discusses the results obtained for the theoretical calculations of MXene,

4.1 Structure

Mo_2TiC_2-T_x has a special group of P63/mmc. First pristine system was generated and optimized at 1000k points. Due to the presence of transition elements and their correlation DFT+U approach has been made. The lattice parameters of the pristine unit cell are a = 2.98Å, b = 2.98Å, c = 36.1Å [20s]. The ground state was achieved by fully relaxing the internal coordinates. Electronic band structure, density of states and the optical properties were then calculated.

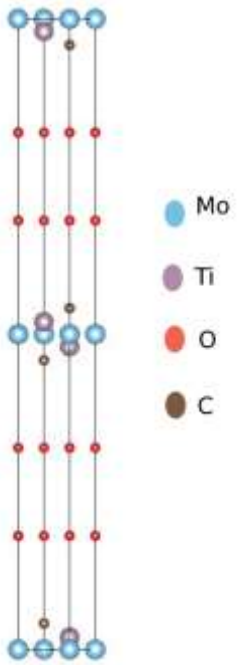

Figure 4.1: *Structure of Pristine $Mo_2TiC_2 – T_x$.*

To study the effects of doping, Nb-doped MXene was simulated using the GGA+U correlations. 4x2x1 super cell was used to study the optical effects of doping of Nb, where it replaces Mo on its Wyckoff sites. The spin polarized calculations were carried out, U indicates the Hubbard potential where U=4eV [22]. U has been applied to the transition elements in the structures i.e., Nb, Ti and Mo. After replacing Molybdenum, the structures internal

coordinates are relaxed and a decrease of the c parameter has been observed compared to the pristine system. With 4% doping of Niobium (Nb) the c parameter shrinks up to 25 Å.

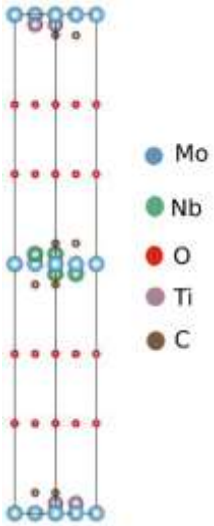

Figure 4.2: *Structure of Nb doped MXene*

4.2 Density of State

Density of states explains the number of states that are available for the energy (eV) in the compound. The DOS per eV and the PDOS for each atom in the structures are shown below.

4.2.1 Pristine System

The DOS for the pristine system are available throughout the region of interest but mostly they are observed between the regions -7.8eV to -3eV, -1ev to 4eV and 5eV to 7eV. This indicates a metallic behavior since there is no energy gap observed.

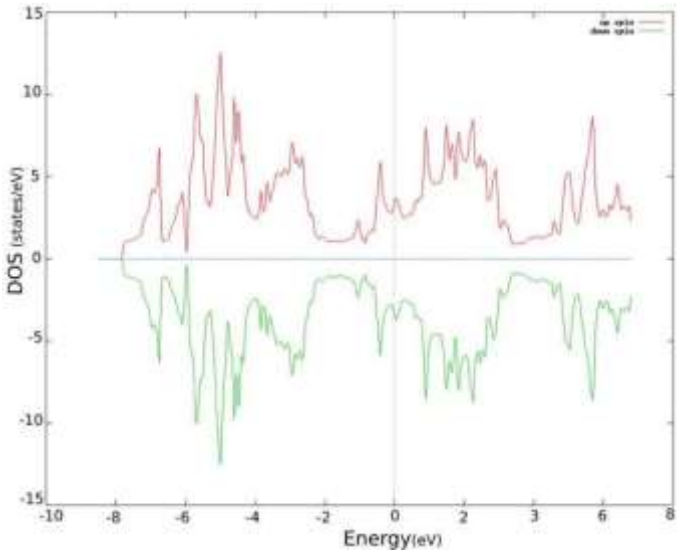

Figure 4. 3: *Total DOS of Pristine Molybdenum MXene*[20].

4.2.2 Nb Doped System

With the introduction of 4% Nb, slight shifting is observed between the spin up and spin down DOS peaks which indicates an introduction of magnetism in the system. Furthermore, the doping also increases the density of states per eV.

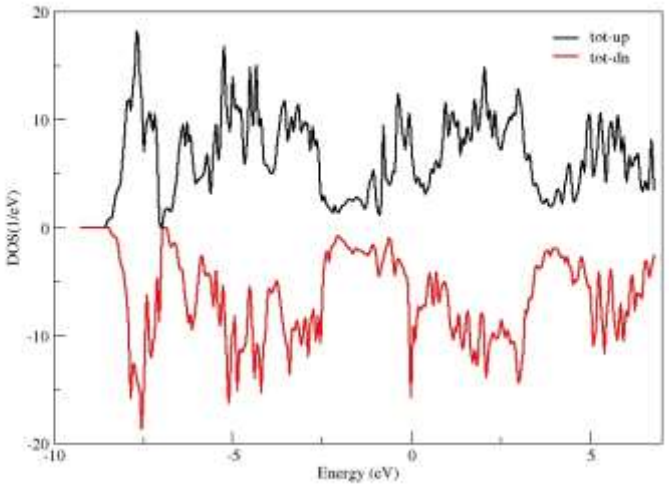

Figure 4. 4: *Total DOS of $MoNbTiC_2T_x$, i.e Nb doped MXene.*

The respective PDOS contributions from each atom have been plotted below in figure 4.5 and slight shifting of the graph can be observed in the PDOS contribution from Nb and Mo.

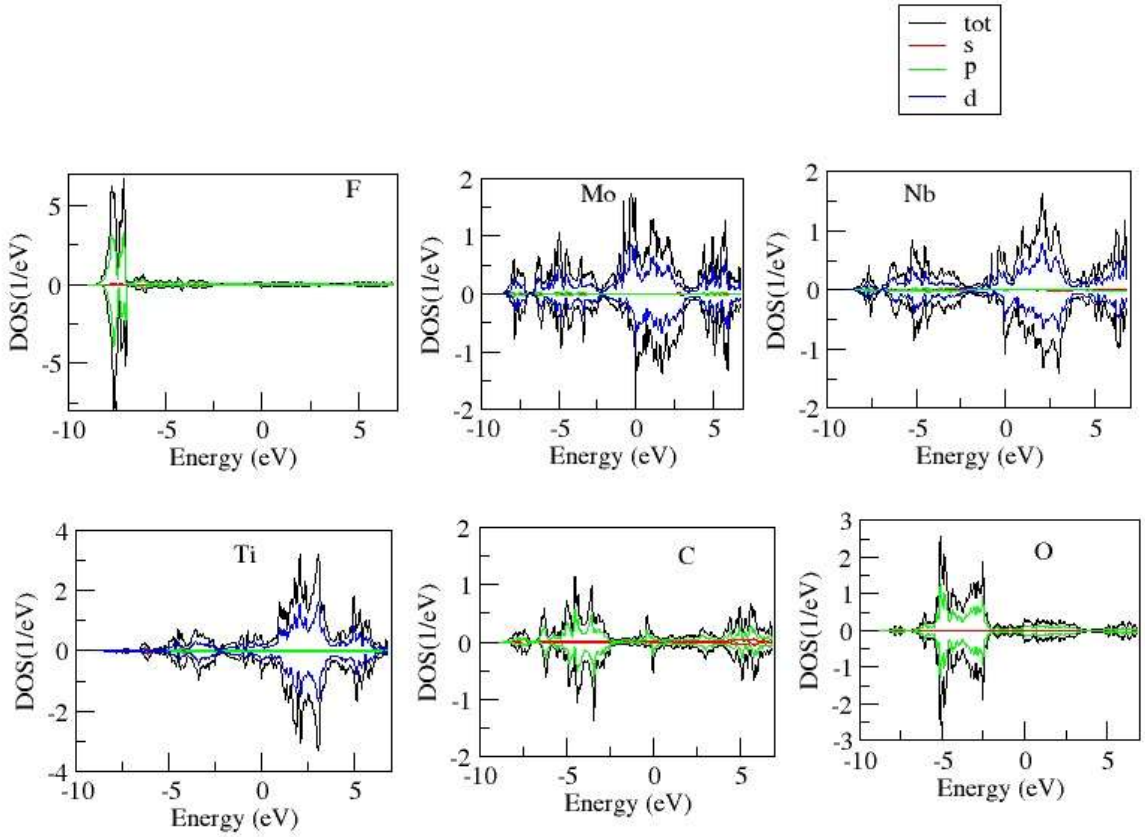

***Figure 4. 5**: Partial DOS contribution of each atom.*

4.3 Magnetic Moment

MXenes, including M_3C_2, have not been extensively researched for their magnetism, both experimentally and theoretically. However, the M_2C phase of compounds like Cr_2C and Ta_2C has been studied and has been found to exhibit various forms of magnetism, including ferromagnetism, anti-ferromagnetism, and ferrimagnetism. This study sheds light on the magnetic behavior of double transition MXenes particularly Mo_2TiC_2-T_x. The overall magnetic moment in Mo_2TiC_2-T_x is 0.0009μB while in the interstitial sites 0.0005μB was observed.

Table 4. 1: *Magnetic contribution from each atom in the unit cell of pristine system*

Atom	Mo (μB)	Ti (μB)	C (μB)
Magnetic-Moment	0.00103	0.00021	0.00020

It has been observed that the introduction of Nb to the pristine system causes rise of magnetic behavior in the lattice. Although Niobium doesn't show a magnetic behavior independently, but after doping into MXene, it gives rise to the magnetic moment. This effect might be arising due to the exchange interactions between Nb and Mo that align the valence shell electrons in a particular direction. The total magnetic moment observed is 4.23819 μB while the interstitial sites show a magnetism of 1.26056 μB.

Table 4. 2: *Magnetic contribution from each atom in the unit cell of the Nb doped MXene.*

Atom	Mo1 (μ_B)	Mo2 (μ_B)	Nb1 (μ_B)	Nb2 (μ_B)	Ti1 (μ_B)	Ti2 (μ_B)	C (μ_B)
Magnetic-Moment	0.58860	0.53991	0.08912	0.06931	0.02157	0.01082	0.02883

From these results, it can be observed that the correlation between Mo and Nb results in the greatest atomic contribution towards the net magnetism of the crystal. Here Mo1 and Mo2 are those atoms which form a bonding with the two Niobium atoms.

4.4 Band structure

Band structure diagrams depict the quantum mechanical behavior of the electrons inside the solids. The bandgap for both doped and un-doped system was 0 eV, which depicts a conductive behavior. The number of electron energy orbitals available close to the Fermi Energy lever increase with the doping of Nb, which implies of an increase in the conductive behavior of the material.

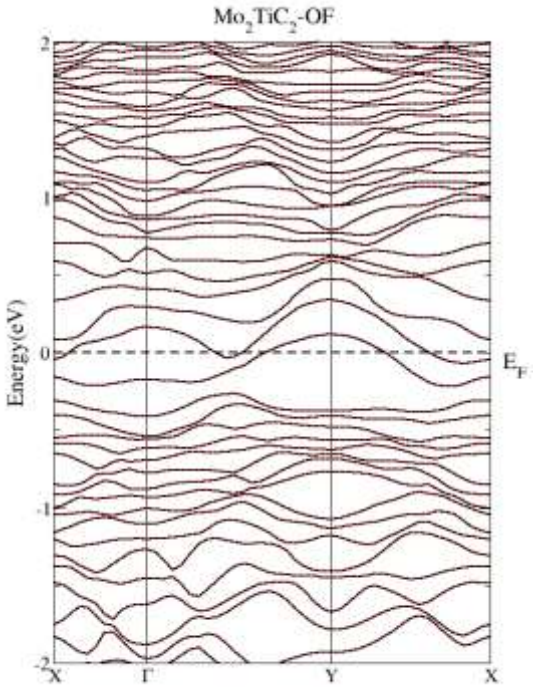

Figure 4. 6: *Band structure of Mo_2TiC_2-T_x*

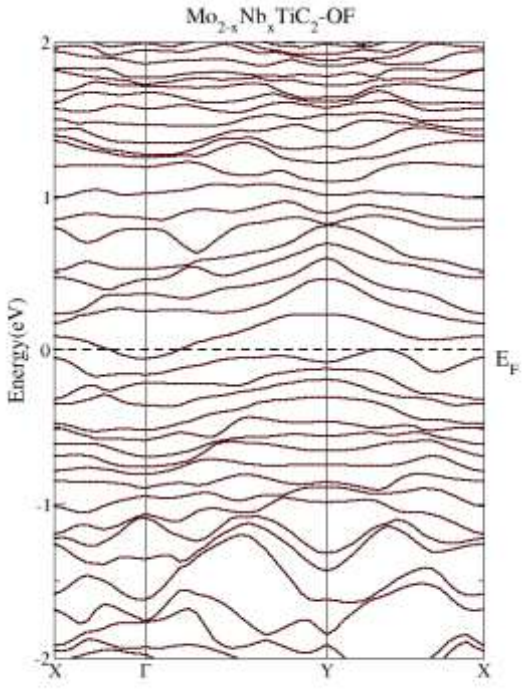

Figure 4. 7: *Bandstructure of MoNbTiC-Tx*

4.5 Optical Properties

Light interacts with matter in a variety of ways. Optical characteristics refer to a substance's response to electromagnetic radiation, and optical materials are substances that can be affected by the flow of light. Every substance has its own unique optical properties; some absorb certain colors of light while others reflect or scatter light in different ways. For example, metals tend to have a shiny appearance, while glass is transparent. Metals typically reflect all wavelengths of light up to ultraviolet, while insulators are dielectrics that are transparent to visible light and semiconductors are often opaque to visible light but transparent to ultraviolet light. The optical properties of a substance are determined by its structural properties and chemical composition, which can vary from one material to another. The optical characteristics of solids can be used to study energy band structure, impurities, defects, and lattice vibrations. In this section, we will briefly review the concepts of absorption, reflection, and transmission. When light hits a medium, it can be reflected, transmitted, or propagate through it. We will first discuss the relationship between optical absorption and absorption coefficient, followed by complex dielectric functions and optical conductivity, and the relationship between the energy band structures of solids.

4.5.1 Optical Absorption

Optical absorption is the process by which a material absorbs electromagnetic radiation, or light. The ability of a material to absorb light is influenced by its characteristics and occurs when the frequency of the light matches the natural resonance frequency of the material's dipole oscillators. When this happens, the dipole oscillators absorb a portion of the energy from the incoming light, while the remainder is released as heat. In the following illustration, the energy of the valence band is represented by E_v, the energy of the conduction band is represented by Ec, and the energy of the bandgap is represented by Eg. When a photon with an energy of hf encounters the substance, two processes can occur:

1. If the energy of the photon, hf, is greater than the energy of the bandgap, Eg, the electron in the valence shell absorbs energy and becomes excited. This causes the electron to move from a lower energy level to a higher one, creating an electron-hole pair in the valence and conduction bands. However, due to scattering, the excited electron loses energy to the lattice and returns to the valence band, where it recombines with the hole.

2. If the energy of the photon, hf, is less than the energy of the bandgap, Eg, the excitation process does not occur. This can make certain materials transparent within a specific range of wavelengths.

4.5.2 The Complex Dielectric Function and Complex Optical Conductivity

The complex dielectric function is a mathematical function that characterizes how a material responds to an applied electric field. It is usually represented by the symbol ε(ω), where ω is the angular frequency of the applied field. The complex dielectric function can be expressed as a complex number with a real and imaginary component. The real part of the complex dielectric function, denoted by ε'(ω), describes the material's ability to absorb or reflect light, while the imaginary part, denoted by ε"(ω), describes the material's ability to scatter-light.

This can be derived from the Maxwell's equations as following:

$$\nabla^2 E = \frac{\varepsilon\mu}{c^2}\frac{\partial 2E}{\partial t^2} + \frac{4\pi\sigma\mu}{c^2}\frac{\partial E}{\partial t} \tag{4.1}$$

$$\nabla^2 H = \frac{\varepsilon\mu}{c^2}\frac{\partial 2H}{\partial t^2} + \frac{4\pi\sigma\mu}{c^2}\frac{\partial H}{\partial t} \tag{4.2}$$

The quantity in the previous equations introduces the notion of the complex dielectric function.

To solve equations above, we need a sinusoidal solution.

$$E = E_O e^{-i(K.r-\omega t)} \tag{4.3}$$

The complex propagation constant, K, and the angular frequency of the light, ω, can be used to find the wave solution for H. The real component of K represents the wave vector, while the imaginary component represents wave attenuation in solids. Substituting the wave solution into the given equation using the value of the wave vector yields the following expression:

$$-K^2 = \frac{-\varepsilon\mu\omega 2}{c^2} - \frac{4\pi i\sigma\mu\omega}{c^2} \tag{4.4}$$

The second expression of equation above vanishes if there is no attenuation in solids, then the equation above becomes:

$$K_0 = \frac{\omega}{c}\ \sqrt{(\varepsilon_{complex}\ \mu)} \tag{4.5}$$

ε is however a real function of K, it also contains a loss factor, therefore the dielectric function may be represented as follows in terms of real and complex parts:

$$\varepsilon complex = \varepsilon + \frac{4\pi i\sigma}{\omega} = \varepsilon 1 + i\varepsilon 2 \tag{4.6}$$

$$\varepsilon_{complex} = \frac{4\pi i\sigma}{\omega} + \frac{\varepsilon\omega}{4\pi i} \tag{4.7}$$

We may define complex conductivity using equation above:

$$\sigma_{complex} = \sigma + \frac{\varepsilon\omega}{4\pi i} \tag{4.8}$$

For the matter-light interaction in the quantum regime, the perturbation is incorporated. Into the system and the expression for the dielectric function takes the following form:

$$\varepsilon(\omega) = \ \varepsilon_1(\omega) + i\varepsilon_2(\omega) \tag{4.9}$$

First the imaginary part is determined and then using the Krammers-Krong relationship which is given in[21].

$$\varepsilon_2(\omega) = \frac{Ve^2}{2\pi\hbar m^2\omega^2}\int d^3k \sum_{n,m} |< kn|\ p\ |kn >|^2\, f(kn)$$

$$\times\,[1 - f(kn)]\,\partial(E_{kn} - E_n - \hbar\omega) \tag{4.10}$$

$$\varepsilon_1(\omega) = 1 + \frac{2}{\pi}\int_0^\infty \frac{\varepsilon_2(\omega)\omega d\omega}{\omega - \omega'} \tag{4.11}$$

4.5.3 Refractive Index

The refractive index is a measure of the material's ability to bend light and is dependent on the wavelength of the light. It is a combination of both real and imaginary parts and can be represented as follows:

$$Ncomplex = \sqrt{\mu\varepsilon complex} \tag{4.12}$$

The relationship between the K and N complex may be described as follows [22]:

$$K = \frac{\omega}{c} Ncomplex \tag{4.13}$$

Now we will write N complex in terms of real and complex function.

$$Ncomplex = n + ik \tag{4.14}$$

Due to the changing dynamics at the nanoscale, the Krammers-Krong relationship is used to compute the dielectric functions thus both components of the refractive index take the following form [22].

$$n(\omega) = \frac{1}{\sqrt{2}} [\sqrt{\varepsilon_1(\omega)^2 + \varepsilon_2(\omega)^2} + \varepsilon_1(\omega)]^{1/2} \tag{4.15}$$

4.5.4 Absorption Coefficient

The absorption coefficient, α, is a measure of how much light is absorbed by an optical material. It is defined as the percentage of energy absorbed per unit length of the medium. When incident light from a monochromatic source hits an optical medium, a portion of the photon's energy is absorbed if the energy of the photon, hf, is greater than the energy of the bandgap, E_g. The remainder of the energy is transmitted through the medium. If the beam is traveling in the x-direction and the intensity at a position 'x', is I(x), the intensity will decrease by an incremental slice of thickness dx due to absorption as follows:

$$I(x) \propto -\left(\frac{dI(x)}{d(x)}\right) \tag{4.16}$$

$$I(x) = -\alpha \frac{dI(x)}{d(x)} \tag{4.17}$$

Equation has the following solution:

$$I(x) = Ioe^{-\alpha x} \tag{4.18}$$

The intensity of the light hitting on the substance is measured in Io. Similarly, the residual intensity of the transmitted light after incident light passes through the medium may be stated as:

$$I_t(x) = Ioe^{-\alpha x} \tag{4.19}$$

$$I_t(x)Io = e^{-\alpha x} \tag{4.20}$$

With the graph below, we can observe how the optical absorption coefficient (α) changes as a function of photon energy.

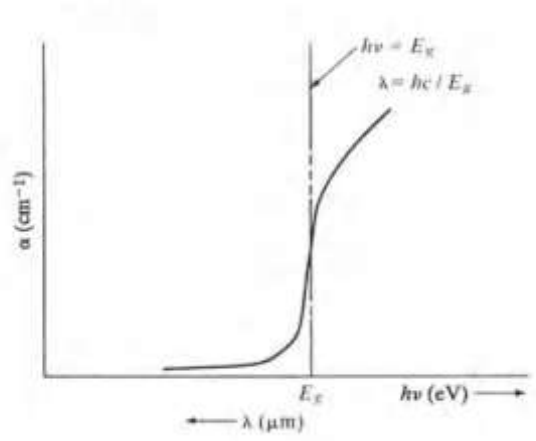

Figure 4. 8*: Energy vs Absorption.*

In the quantum realm the expression for absorption takes the following form

$$\boldsymbol{\alpha} = \sqrt{2\omega}\left[\sqrt{\varepsilon_1(\omega)^2 + \varepsilon_2(\omega)^2} - \varepsilon_1(\omega)\right]^{1/2} \tag{4.21}$$

4.5.5 Reflectivity

Reflectivity is a characteristic of a material that describes how much light is reflected off its surface when compared to the amount of incident light. The diagram in Figure 4.8 shows a schematic of an optical system. It is assumed that the material in the figure is thick enough to absorb light. If we disregard the reflection from the back of the material, the one-dimensional propagating wave can be expressed as follows:

$$Ex = E_o e^{-i(K.r-\omega t)} \tag{4.21}$$

In equation above, K is the complex propagation constant, which has previously been determined.

Both incident and reflected waves exist in free space:

$$Ex = E_1 e^{-i(\omega zc-\omega t)} + E_2 e^{-i(-\omega zc-\omega t)} \tag{4.22}$$

The continuity of E_x may be connected to the following equation using equations given above

$$E0 = E_1 + E_2 \tag{4.23}$$

We may get the following relationship from the Maxwell relation:

$$\frac{\partial Ex}{\partial z} = \frac{i\mu\omega}{c} Hy \tag{4.24}$$

Using equations above, we get

$$E_0 K = \frac{E_1\omega}{c} - \frac{E_2}{c} = \frac{E_0\omega}{c} N_{complex} \tag{4.25}$$

$$E_1 - E_2 = E_0 N_{complex} \tag{4.26}$$

R is now defined as the perpendicular incident reflectivity.

$$R = \frac{E_2}{E_1} \tag{4.27}$$

We are now familiarizing with reflection coefficient r given by

$$r = \frac{E_2}{E_1} \tag{4.28}$$

The following are the outcomes of above equations.

$$E_2 = \frac{1}{2} E_0 \, (1 - N_{complex}) \tag{4.29}$$

$$E_1 = \frac{1}{2} E_0 \, (1 + N_{complex}) \tag{4.29}$$

The perpendicular incident reflectivity has now obtained the form.

$$R = \frac{1 - N_{complex}^2}{1 + Ncomplex} = \frac{((1-n)^2 + k^2)}{(1+n)^2 + k^2} \tag{4.31}$$

A property called reflectivity R, which is important in optics, has been added. The power transmitted or absorbed by a material when light is incident on it at a right angle can be determined using the relationship mentioned.

$$1 = A + R + T \tag{4.32}$$

At the quantum mechanical scale, the expressions change as following [22].

$$R(\omega) = \left(\frac{\sqrt{{\varepsilon_1}^2 + j{\varepsilon_1}^2} - 1}{\sqrt{{\varepsilon_1}^2 + j{\varepsilon_1}^2} + 1} \right)^2 \tag{4.33}$$

4.5.6 Optical Loss

Optical loss is a reduction in the intensity of light as it enters a medium.

$$L(\omega) = \frac{\varepsilon_2(\omega)}{\varepsilon_2(\omega)^2 + \varepsilon_1(\omega)^2} \tag{4.34}$$

The occurrence of optical losses happens when light, which has the potential to create an electron hole pair, does not generate any because it gets reflected from the front surface.

4.5.7 Optical Conductivity

Optical conductivity is a measure of how well a material allows light to pass through it. Materials with high optical conductivity are transparent or translucent, while materials with low optical conductivity are opaquer. The optical conductivity of a material can be affected by factors such as its type, purity, and the presence of impurities or defects. It is used in various fields such as telecommunications, solar cells, and display technology.

$$\sigma = \frac{\omega}{4\pi}\varepsilon_2(\omega) \tag{4.35}$$

4.6 Optical Properties of Mo2TiC2-Tx and MoNbTiC2-Tx

To study the effects of interaction of field with our systems, 4x2x1 supercell was created and all of the optical properties were calculated.

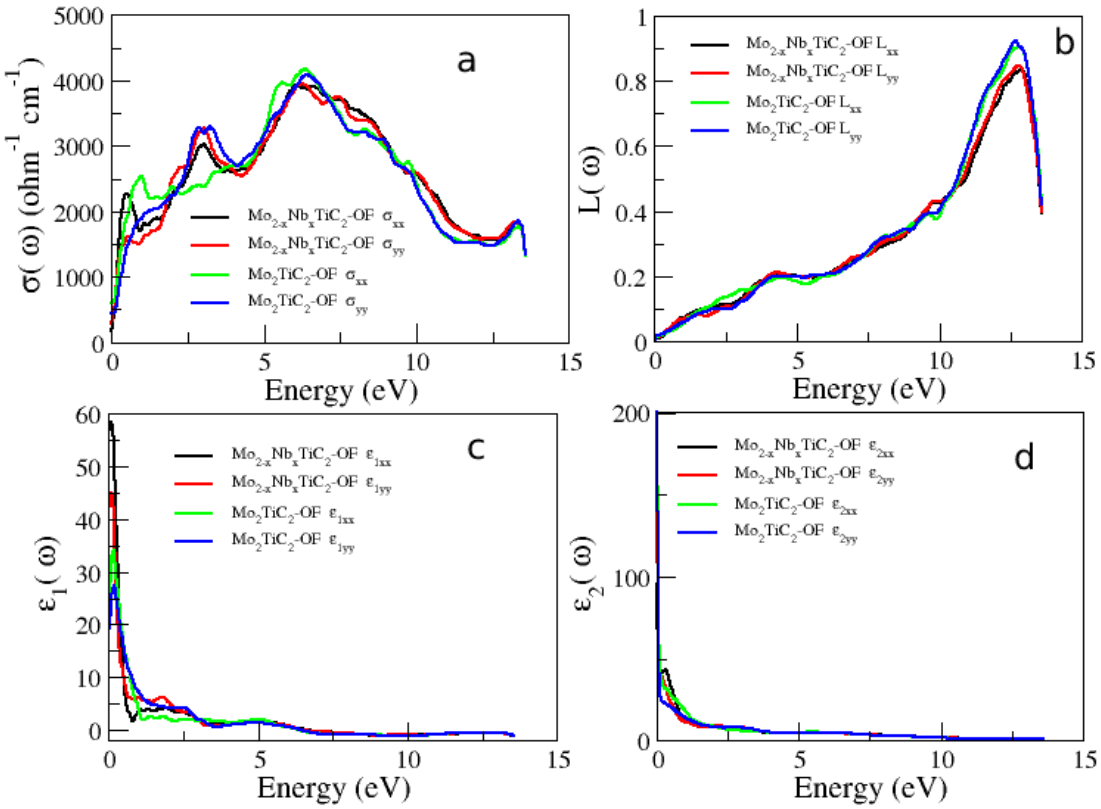

Figure 4.9: *Comparison of the Optical conductivity (a), Optical loss (b) and both dielectric components of both (c), (d) of the materials under study.*

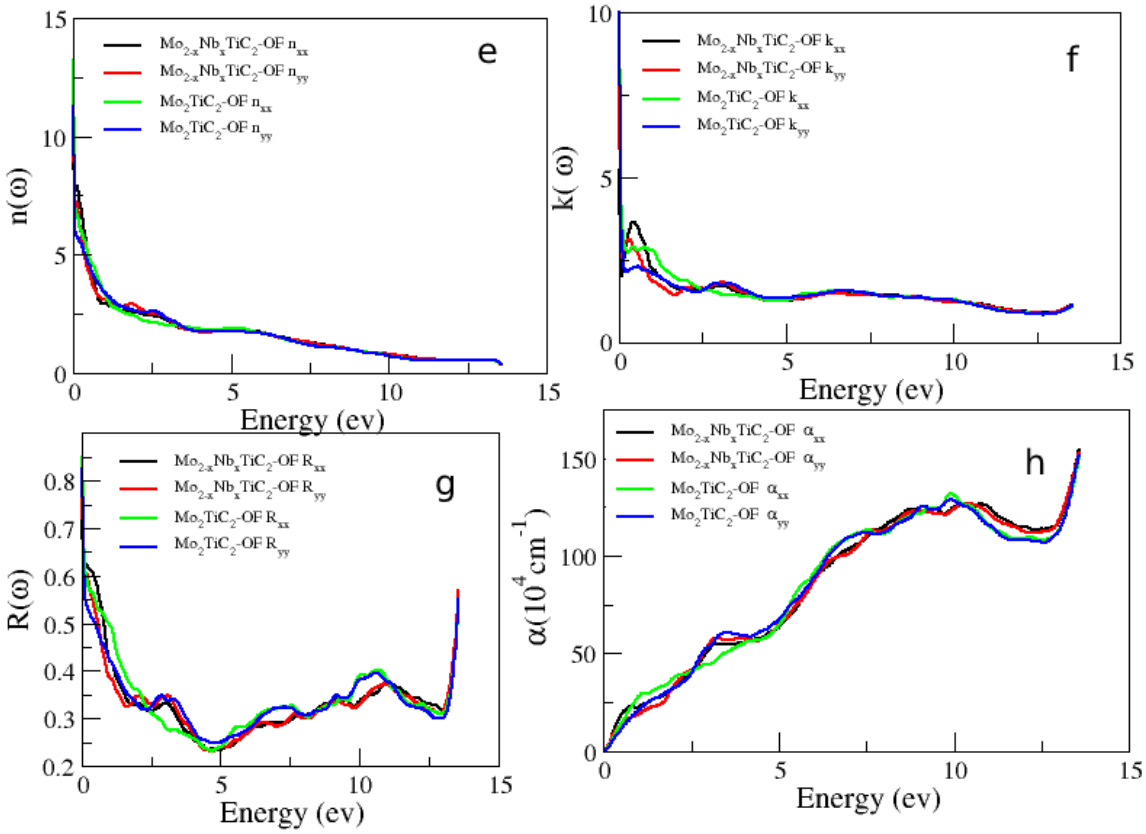

Figure 4.10: *Comparison of Refractive Index (e), Absorption (f), Reflectivity(g) and Extinction Coefficient (h).*

From the calculations, the optical behavior of both materials is found to be very similar.

- In both systems, high **optical absorption** has been reported especially in the regions of higher frequency of the electromagnetic wave. It can be seen in 4.10 (h), the absorption increases along with the increase in the electromagnetic frequency, and due to this there is a potential of these materials to find their applications in solar cell fabrication.
- In the visible region i.e., till 3eV, the **optical conductivity** has an ascending trend in the figure 4.10(a). This is another feature which indicates that this material shows promising characteristics for applications in solar cells. After entering the UV region, the conductivity has a downward trend after 6.5 eV.
- **Optical loss** indicates an ascending trend. From figure 4.10 (b) it can be observed that optical loss increases across IR, Visible and the UV region. Loss peaks at 12.7 eV energy of the incident wave this means that both systems can carry the light waves up to 12.7 eV intensity with least distortion.

- The figure 4.10 (g) indicates that the **Reflectivity** of the system shows a downward trend and hits the bottom at 5eV, after that it increases again and shows some stability. At 14eV the reflectivity peaks again. One explanation for such a behavior is that, due to the rise in the lattice vibrations, the momentum from the incident EM wave scatters inside the lattice, giving rise to a greater number of phonons, which result in the higher absorption of light, causing a decrease in the ability of the material to reflect.
- The real component of the refractive index indicates the change in wavelength or velocity of a wave as it transitions from vacuum to medium, whereas the imaginary part depicts the wave's attenuation in the medium.

  $$N = n + ik$$

  From the figure 4.10 (e) and 4.10 (f) it can be seen that the system under consideration experiences decreases in the real and imaginary component of the refractive index (**Extinction Coefficient**).

- From the figure 4.10 (c) and 4.10 (d), it is observed that the both components of the dielectric function are decaying with the increase of the energy of the light wave.

Chapter 5
Conclusion

In this study, density functional theory has been incorporated for the computational study of $Mo_2TiC_2–T_x$ and $MoNbTiC_2$-T_x. The study shows that both of the systems are electrically conductive in nature. With the 4% doping in the pure MXene, magnetic effects have been observed. Furthermore, optical properties have also been studied, which were observed to be very similar for both systems under study and it has been predicted that both materials have a potential to find their application in the solar cell fabrication.

5.1 Future Directions

Even though this thesis may contain digressions, it still offers some areas for exploration and examination through experimentation. For instance, there is a need to optimize the fabrication approach for creating solar cells from both systems. Additionally, since doping of Nb in the system predicts magnetism, there is potential for applications in magnetism and spintronics, and further testing is needed to assess its potential in those areas.

References

1. Han M, Shuck CE, Rakhmanov R *et al.* Beyond Ti3C2Tx: MXenes for Electromagnetic Interference Shielding. ACS Nano 2020; 14: 5008–5016.

2. Shinde PA, Patil AM, Lee S, Jung E, Chan Jun S. Two-dimensional MXenes for electrochemical energy storage applications. J Mater Chem A 2022; 10: 1105–1149.

3. Lim KRG, Shekhirev M, Wyatt BC, Anasori B, Gogotsi Y, Seh ZW. Fundamentals of MXene synthesis. Nature Synthesis 2022; 1: 601–614.

4. Han M et al. Tailoring Electronic and Optical Properties of MXenes through Forming Solid Solutions. ournal of the American Chemical Society 142,45 (2020):

5. Anasori B, Xie Y, Beidaghi M *et al.* Two-Dimensional, Ordered, Double Transition Metals Carbides (MXenes). ACS Nano 2015; 9: 9507—9516.

6. Gao Y, Cao Y, Zhuo H *et al.* Mo2TiC2 MXene: A Promising Catalyst for Electrocatalytic Ammonia Synthesis. Catal Today 2018; 339.

7. Chen X, Li R, Li B *et al.* Achieving ultra-high ductility and fracture toughness in molybdenum via Mo2TiC2 MXene addition. Materials Science and Engineering: A 2021; 818: 141422.

8. Kohn W, Sham LJ. Self-Consistent Equations Including Exchange and Correlation Effects. Phys Rev 1965; 140: A1133–A1138.

9. Board E. Lecture Notes in Physics. .

10. Andjelkovič L, Gruden-Pavlovič M, Daul C, Zlatar M. The choice of the exchange-correlation functional for the determination of the jahn-teller parameters by the density functional theory. Int J Quantum Chem 2013; 113: 859–864.

11. Perdew J, Zunger A. Self-Interaction Correction to Density-Functional Approximations for Many-Body Systems. Phys Rev B 1981; 23: 5048–5079.

12. Perdew JP, Burke K, Ernzerhof M. Generalized Gradient Approximation Made Simple. 1996.

13. 1887_2730301-Article _ Letter to editor. .

14. Blaha P, Schwarz K, Tran F, Laskowski R, Madsen GKH, Marks LD. WIEN2k: An APW+lo program for calculating the properties of solids. Journal of Chemical Physics 2020; 152.

15. Slater JC. Wave Functions in a Periodic Potential. Physical Review 1937; 51: 846–851.

16. Sjöstedt E, Nordström L, Singh D ~J. An alternative way of linearizing the augmented plane-wave method. Solid State Commun 2000; 114: 15–20.

17. Krasovskii EE, Schattke W. The extended-LAPW-based k · p method for complex band structure calculations. Solid State Commun 1995; 93: 775–779.

18. Wimmer E, Krakauer H, Weinert M, Freeman AJ. Full-potential self-consistent linearized-augmented-plane-wave method for calculating the electronic structure of molecules and surfaces: O 2 molecule. Phys Rev B 1981; 24: 864–875.

19. Schwarz K. Computation of Materials Properties at the Atomic Scale. In: Pahlavani MR, editor. Selected Topics in Applications of Quantum Mechanics. Rijeka: IntechOpen, 2015.

20. Anasori B, Shi C, Moon EJ *et al*. Control of electronic properties of 2D carbides (MXenes) by manipulating their transition metal layers. Nanoscale Horiz 2016; 1: 227–234.

21. Fox M. Optical Properties of Solids Second Edition Chapter 1. 2010.

22. Chiu M-H, Lee J-Y, Su D-C. Complex refractive-index measurement based on Fresnel's equations and the uses of heterodyne interferometry. Appl Opt 1999; 38: 4047–4052.